Electronic Supplementary Information

for

Can shock-induced phonon up-pumping model relate to impact sensitivity of molecular crystals, polymorphs and cocrystals?

X. Bidault [1,a)] and S. Chaudhuri [1,2,b)]

[1] *Department of Civil, Materials and Environmental Engineering, University of Illinois at Chicago, Chicago, Illinois 60607, United States*

[2] *Applied Materials Division, Argonne National Laboratory, Lemont, IL 60439, United States*

[a)] Corresponding author: xavbdlt@uic.edu

[b)] Electronic mail: santc@uic.edu

1. Evaluation of the "nitroaromatics" model for nitramines

The model of Deng *et al.* [1] was devised to predict shock sensitivity of nitroaromatics, using molecular descriptors (the numbers nC, nH, nN and nO of Carbon, Hydrogen, Nitrogen and Oxygen atoms, respectively, the Oxygen balance OB and the molecular weight MW) and a crystal descriptor (the bulk modulus). Definitions and formulas can be found in their paper. Their Equation (13) is the one used to predict h_{50}:

$$log_2 h_{50} = 3.65\frac{OB.MW}{nH - MW} + 3.4\frac{\sqrt[3]{nO}}{nN.K} + 0.72\frac{nH.\sqrt[2]{K}}{nC} + 3.3$$

Presently, the bulk modulus is derived from DFT-D calculations, using Quantum Espresso, PBE-D2, PSlib 1.0.0 US PP with a cutoff of 90 Ry (more details can be found in Section II.A. of the manuscript). Using variable-cell relaxation at -2, 0 and +2 kbar, the bulk modulus is calculated as

$$K_T = -V_0\frac{\partial P}{\partial V}$$

where V_0 is the volume at 0 kbar, and the differential term is approximated by the finite differences between values at -2 and +2 kbar. This method using PBE-D2 and PP was already shown to yield lattice parameters very close to values at ambient conditions [2] (see also Table SIII). The calculated bulk modulus is thus considered at ambient conditions. The results are reported in Table SI. The density and bulk modulus are indeed close to known ambient experimental data. While h_{50} is rather well predicted for aromatic nitramine (TATB and TNT), very large errors appear for non-aromatic nitramines. FOX-7 is found much less sensitive than TATB, and β-HMX even less, with its h_{50} higher than 800 cm. Going deeper and considering polymorphs, this model

erroneously predicts β- and δ-HMX similarly insensitive, whereas both are experimentally sensitive, and δ-HMX even more than β-HMX [3]. Then, β- and ε-CL20 are predicted with sensitivity similar to TNT, whereas both are experimentally more than that, and β-CL20 more than ε-CL20 [4]. This model lacks of transferability and obviously needs a parameterization for nitramines.

Table SI. Sensitivity prediction from the "nitroaromatics" model applied to a few nitroaromatics and nitramines. The deviation *(%dev)* of density and bulk modulus are in reference to ambient experimental data found in [2]. The deviation *(%dev)* of h_{50} is in reference to experimental data reported in the main manuscript.

	MW	**OB**	**Density** *(%dev)*	**K (GPa)** *(%dev)*	**log2(h_{50})**	**h_{50} (cm)** *(%dev)*
TATB ($C_6H_6O_6N_6$)	268.15	-0.5370129	1.975 *(+1.9)*	13.3 *(+2.6)*	8.01	**258** *(-47)*
o-TNT ($C_7H_5O_6N_3$)	227.15	-0.7395994	1.65*	6.77*	6.29	**78.4** *(+48/-23)*
α-FOX-7 ($C_2H_4O_4N_4$)	148.08	-0.2160994	1.915 *(+1.1)*	13.1 *(+4.0)*	9.42	**685** *(+444)*
β- HMX ($C_4H_8O_8N_8$)	296.155	-0.2161030	1.911 *(+0.6)*	15.3 *(+3.9)*	9.79	**886** *(+2585)*
δ-HMX ($C_4H_8O_8N_8$)	296.155	-0.2161030	1.777	14.7	9.69	**827**
ε-CL20 ($C_6H_6O_{12}N_{12}$)	438.185	-0.1095428	1.997 *(-2.3)*	11.5 *(-4.6)*	6.20	**73.5** *(+315)*
β-CL20 ($C_6H_6O_{12}N_{12}$)	438.185	-0.1095428	1.959	11.1	6.16	**71.4** *(+449)*
γ-CL20 ($C_6H_6O_{12}N_{12}$)	438.185	-0.1095428	1.886	13.1	6.36	**82.0**
2CL20:1HMX ($C_6H_6O_{12}N_{12}$ + 1/2 $C_4H_8O_8N_8$)	586.25	-0.1364605	1.943	13.7	7.18	**145**

2. Phonon density of states of β-HMX from DFT-D – Issues when using only the Gamma point

The method to calculate the vibrational density of states (vDOS) can be found in Section II.B. of the manuscript and in Ref. [2]. The β-HMX lattice parameters are first optimized at zero pressure using either Quantum Espresso (single cell and 3x2x3 off-grid k-points) or CP2K (2x1x2 supercell and the Gamma point), using various pseudo potentials (PP) and even one all-electron (AE) simulation. The results are reported in Table SII. To determine their phonon density of states, the supercell method as implemented in Phonopy is used on 2x1x2 supercells, large enough for a single k-point. For every DFT-D combination, the respective vDOS are displayed in Fig. S1. It shows evidence that only the combination using a single cell with the Gamma point (red dotted curve) results in a vDOS which strongly differs from the other combinations, especially in the low-frequency range and with significant negative frequencies. This choice could fit high-throughput considerations, concerning fast calculations, but the lattice/intermolecular vibrations are poorly described. We consider this an

issue when quantifying shock sensitivity based on an up-pumping scheme from the phonon bath. For this reason, we avoided in the present study this less accurate and cheap combination.

Table SII. β-HMX unit-cell from variable-cell relaxation using different DFT-D methods. The *italic* value under every lattice parameter is the percentage deviation *%dev* from the experimental data at 303 K taken from ref. CCDC 792930. QE uses a single cell with a mesh of 3x2x3 off-grid k-points. CP2K uses a 2x1x2 supercell and the Gamma point. NLCC is used for all PP.

						a (Å)	b (Å)	c (Å)	β (°)	V (Å^3)
Exp.						**6.526**	**11.037**	**7.364**	**102.67**	**517.45**
QE	PBE-D2	PP	PSlib1.0.0	90 Ry	3x2x3 (off-grid)	6.560	10.856	7.404	102.60	514.53
%dev						*+0.5*	*-1.6*	*+0.5*	*-0.1*	*-0.6*
QE	PBE-D2	PP	PseudoDojo Std	120 Ry	3x2x3 (off-grid)	6.547	10.905	7.224	102.56	512.35
%dev						*+0.3*	*-1.2*	*-1.9*	*-0.1*	*-1.0*
QE	PBE-D2	PP	ONCV 1.2	400 Ry	3x2x3 (off-grid)	6.551	10.907	7.239	102.62	512.22
%dev						*+0.4*	*-1.2*	*-1.7*	*-0.0*	*-1.0*
CP2K	PBE-D2	PP	GTH-mTZVP	1500 Ry	Superc. 2x1x2 + Gamma	6.556	10.915	7.366	102.67	514.30
%dev						*+0.5*	*-1.1*	*+0.0*	*0.0*	*-0.6*
CP2K	PBE-D3(BJ)	AE	AE 6-311G**	1500 Ry	Superc. 2x1x2 + Gamma	6.548	10.900	7.291	102.90	507.25
%dev						*+0.3*	*-1.2*	*-1.0*	*+0.2*	*-2.0*

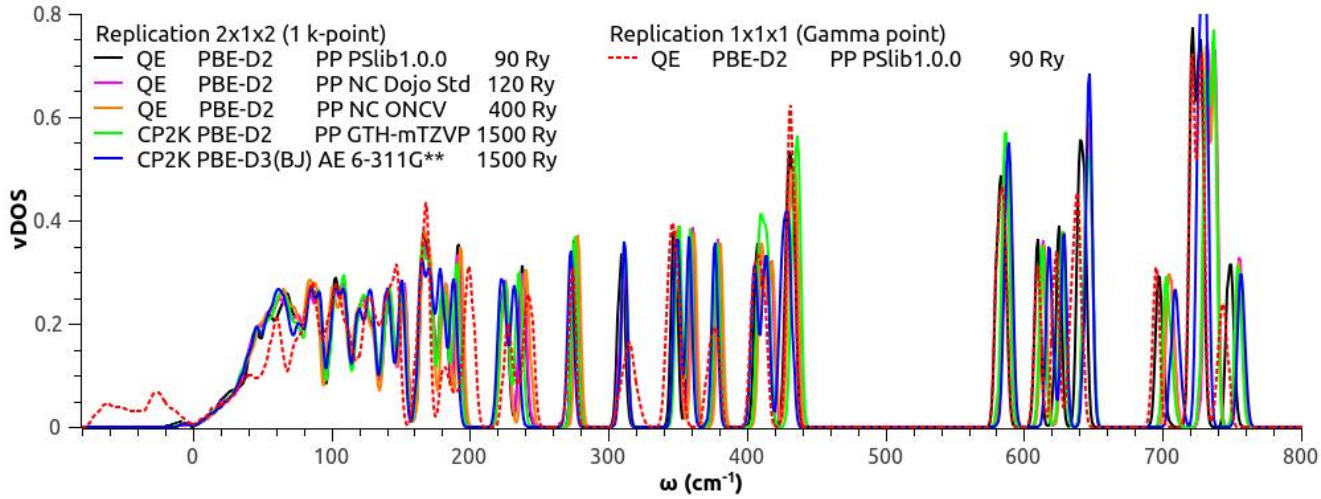

Fig. S1. Phonon density of states of β-HMX using various DFT-D combinations, from the structures optimized in Table SII. The quick calculations using a single cell and only the Gamma point for the phonon calculations is also the less accurate (red dotted curve). The other combinations agree very well with each other.

3. Additional QE and PHONOPY simulation parameters

Table SIII. Monkhorst-Pack parameters for variable-cell optimization of the unit cell, supercell size for phonon calculations, and resulting phonon bath extent ω_{max} from phonon analysis (including highest X-NO_2 twisting modes).

	Monkhorst-Pack off-grid k-point mesh	Supercell (unit cell replication)	Molecules in the supercell	Atom total	Irreducible representations	ω_{max} (cm^{-1})
PETN-I	2x2x3	2x2x2	16	464	44	125
BTF	3x1x3	2x1x2	16	288	108	153
β-HMX	3x2x3	2x1x2	8	224	84	176
δ-HMX	3x3x1	2x2x1	24	672	168	152
α-NTO	4x3x2	3x2x1	48	528	264	171
HNB	2x3x3	2x2x2	32	768	72	166
Tetryl	2x3x2	2x2x2	32	800	150	204
HNAB	2x4x2	1x3x1	12	432	432	213
HNS	1x4x2	1x3x1	12	456	228	217
DIPAM	3x2x1	2x1x1	8	288	216	227
TNB	2x1x2	2x1x2	64	1152	216	152
MATB	4x3x2	3x2x1	24	480	120	161
DATB	3x4x2	2x3x1	12	264	132	181
TATB	2x2x3	2x2x2	16	384	144	133
α-FOX-7	3x3x2	2x2x1	16	224	84	172
α-CL20	3x2x1	2x1x1	16	576	216	153
β-CL20	2x2x2	2x2x2	16	576	216	158
γ-CL20	2x2x2	2x2x2	16	576	216	199
ε-CL20	2x2x2	2x2x2	16	576	216	178
MTNP	2x3x3	1x2x2	16	288	108	173
2CL20:1HMX	1x2x2	1x2x2	16 + 8	800	300	166
1CL20:1MTNP	3x2x2	2x1x1	4 + 4	216	324	190

4. Comparison of the theoretical phonon vDOS to experimental INS spectra

Fig. S2 compares our calculated vDOS of β-HMX, α-NTO, TATB and α-FOX-7 to experimental spectra of inelastic neutron scattering (INS) performed at 20 K [5][6]. Peak positions agree within 3%. The largest relative deviation (8%) occurs at the upper part of the phonon bath of α-FOX-7 (170 cm^{-1}), which is good for this challenging low-frequency range [7]. Our all-electron calculations improve this range for α-FOX-7 (blue curve in Fig. S2). Even though strong similitudes can be seen in the low-frequency range, we recall that a straight comparison of shape and intensity would require calculating neutron instead of phonon spectra.

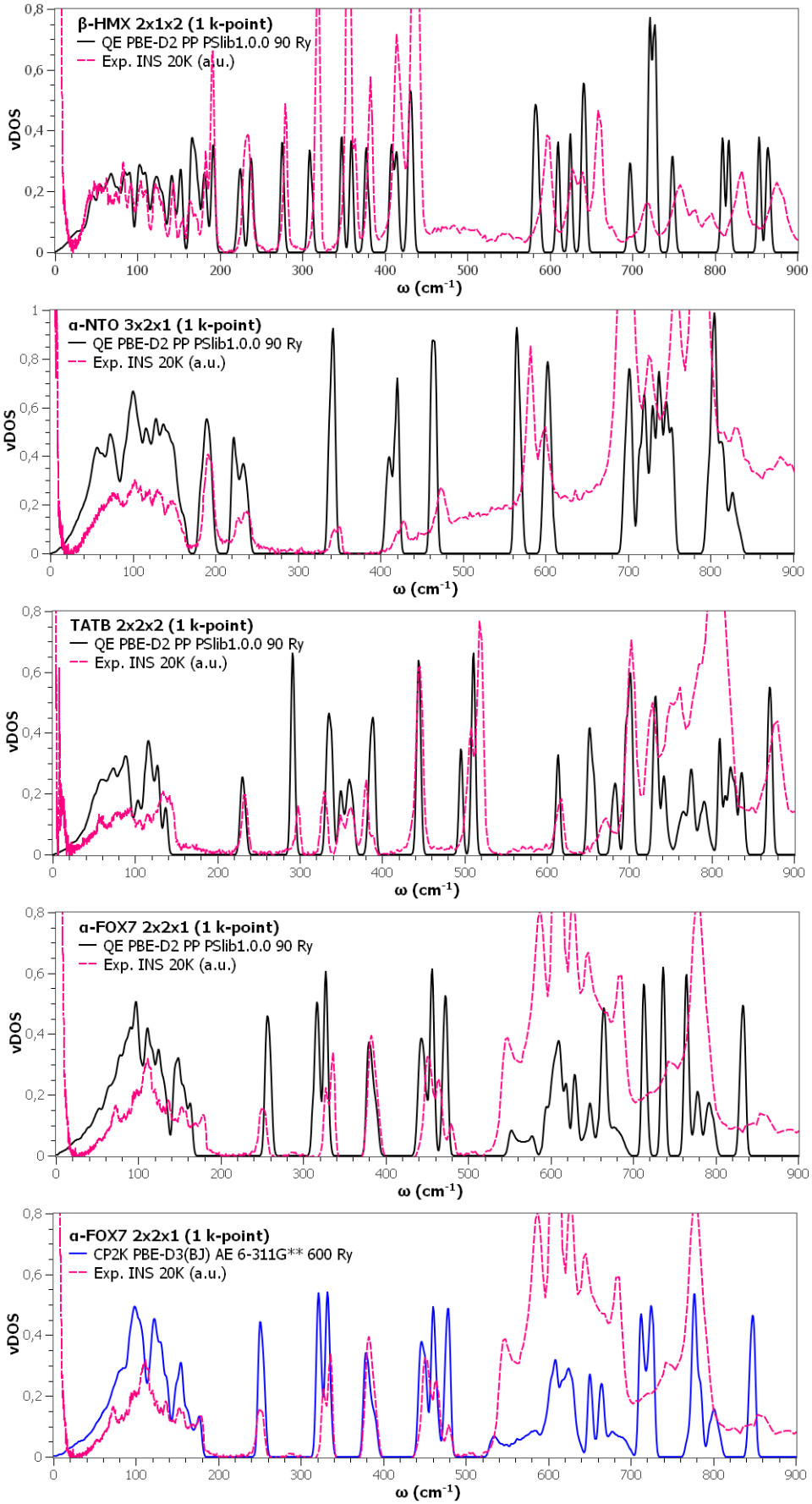

Fig. S2. Comparison of the theoretical phonon vDOS of β-HMX, α-NTO, TATB and α-FOX-7 to experimental spectra of inelastic neutron scattering performed at 20 K [5][6].

5. Optimized lattice parameters from DFT-D

Table SIV reports the results of the variable-cell relaxation as performed in section II.A. of the manuscript. The resulting structures agree very well with data at ambient conditions.

TABLE SIV. PBE-D2 optimizations at 0 K and 0 bar, using PSlib 1.0.0 US pseudopotential and 90 Ry energy cutoff.

Name Grp. Sym. CCDC ref.		a (Å)	b (Å)	c (Å)	α (°)	β (°)	γ (°)	V (Å^3)	ρ (g/cm^3)
β-HMX	Exp. 303K	6.526	11.037	7.364		102.67		517.45	1.901
$P2_1/n$	PBE-D2	6.560	10.856	7.404		102.60		514.53	1.912
792930	*% dev*	*+0.5*	*-1.6*	*+0.5*		*-0.1*		*-0.6*	*+0.6*
δ-HMX	Exp. 295K	7.711		32.553			120.00	1676.27	1.760
$P6_1$	PBE-D2	7.629		32.956			120.00	1661.15	1.776
1225493	*% dev*	*-1.1*		*+1.2*			*0.0*	*-0.9*	*+0.9*
α-FOX7	Exp. 298K	6.934	6.623	11.312		90.06		519.47	1.893
$P2_1/n$	PBE-D2	7.005	6.484	11.309		90.96		513.6	1.915
616838	*% dev*	*+1.0*	*-2.1*	*-0.0*		*+1.0*		*-1.1*	*+1.1*
PETN-I	Exp. 295K	9.386		6.715				591.57	1.774
$P\text{-}42_1/n$	PBE-D2	9.390		6.669				588.03	1.785
1231269	*% dev*	*+0.0*		*-0.7*				*-0.6*	+0.6
ε-CL20	Exp. Amb.	8.852	12.556	13.386		106.82		1424.15	2.044
$P2_1/n$	PBE-D2	8.939	12.661	13.428		106.46		1457.52	1.997
117779	*% dev*	*+1.0*	*+0.8*	*+0.3*		*-0.3*		*+2.3*	*-2.3*
β-CL20	Exp. 293K	9.676	13.006	11.649				1465.98	1.985
$Pb2_1/a$	PBE-D2	9.682	13.301	11.553				1485.98	1.959
117777	*% dev*	*+0.1*	*+2.3*	*-0.8*				*+1.4*	*-1.4*
γ-CL20	Exp. 293K	13.231	8.170	14.876		109.17		1518.89	1.916
$P2_1/n$	PBE-D2	13.257	8.303	14.816		108.88		1543.23	1.886
117778	*% dev*	*+0.2*	*+1.6*	*-0.4*		*-0.3*		*+1.6*	*-1.6*
α-CL20	Exp. 293K	9.485	13.225	23.673				2969.52	1.960
Pbca	PBE-D2	9.400	13.467	23.756				3007.10	1.936
117776	*% dev*	*-0.9*	*+1.8*	*+0.3*				*+1.3*	*-1.3*
2CL20:	Exp. 303K	16.346	9.936	12.142		99.23		1946.42	2.001
1HMX	PBE-D2	16.440	9.996	12.376		99.89		2003.69	1.943
$P2_1/n$ 792930	*% dev*	*+0.6*	*+0.6*	*+1.9*		*+0.7*		*+2.9*	*-2.9*
BTF	Exp. 295K	6.923	19.516	6.518				880.64	1.901
$Pna2_1$	PBE-D2	7.010	19.700	6.575				908.04	1.844
1118341	*% dev*	*+1.3*	*+0.9*	*+0.9*				*+3.1*	*+3.0*
α-NTO	Exp. 293K	5.123	10.314	17.998	106.61	97.81	90.13	902.06	1.916
$P\bar{1}$	PBE-D2	5.148	10.422	17.612	107.26	97.67	90.11	893.48	1.934
286331	*% dev*	*+0.5*	*+1.0*	*-2.1*	*+0.6*	*-0.1*	*-0.0*	*-0.9*	*+0.9*
TNB	Exp. 295K	9.78	26.94	12.82				3377.73	1.676
Pbca	PBE-D2	9.571	27.067	12.693				3288.08	1.722
1272828	*% dev*	*-2.1*	*+0.5*	*-1.0*				*-2.7*	*+2.7*
TATB	Exp. 295K	9.010	9.028	6.812	108.58	91.82	119.97	442.52	1.938
$P\bar{1}$	PBE-D2	9.096	9.109	6.606	109.71	91.31	119.94	434.08	1.975
1266837	*% dev*	*+1.0*	*+0.9*	*-3.0*	*+1.0*	*+0.6*	*+0.0*	*-1.9*	*+1.9*

TABLE SIV – cont.

Name Grp. Sym. CCDC ref.		a (Å)	b (Å)	c (Å)	α (°)	β (°)	γ (°)	V (Å^3)	ρ (g/cm^3)
MATB	Exp. 295K	6.137	9.217	15.323		99.67		854.43	1.773
$P2_1/n$	PBE-D2	6.067	9.134	15.451		99.92		843.40	1.797
1272844	*% dev*	*-1.1*	*-0 .9*	*+0.8*		*+0.2*		*-1.3*	*+1.3*
DATB	Exp. 223K	7.309	5.169	11.583		95.22		435.79	1.853
Pc	PBE-D2	7.332	5.196	11.497		93.88		437.00	1.848
	% dev	*+0.3*	*+0.5*	*-0.7*		*-1.4*		*+0.3*	*-0.3*
DIPAM	Exp. **113K**	7.340	11.624	18.734				1598.34	1.825
$P2_12_12_1$	PBE-D2	7.387	11.813	18.824				1642.68	1.776
822227	*% dev*	*+0.6*	*+1.6*	*+0.5*				*+2.8*	*-2.8*
HNB	Exp. 295K	13.220	9.130	9.680		95.55		1162.98	1.988
C2/c	PBE-D2	13.267	9.009	9.768		96.32		1160.30	1.993
1177301	*% dev*	*+0.4*	*-1.3*	*+0.9*		*+0.8*		*-0.2*	+0.2
HNAB	Exp. 298K	15.401	5.524	22.118		110.34		1764.13	1.703
$P2_1$	PBE-D2	15.078	5.747	21.622		110.45		1755.49	1.711
268091	*% dev*	*-2.1*	*+4.0*	*-2.2*		*+0.1*		*-0.5*	*+0.5*
HNS	Exp. 295K	22.326	5.571	14.667		110.04		1713.68	1.745
$P2_1/c$	PBE-D2	21.646	5.621	15.036		112.43		1691.03	1.768
1168120	*% dev*	*-3.0*	*+0.9*	*+2.5*		*+2.2*		*-1.3*	*+1.3*
Tetryl	Exp. 295K	14.129	7.374	10.614		95.07		1101.52	1.731
$P2_1/c$	PBE-D2	14.408	7.234	10.492		96.24		1087.00	1.755
1214794	*% dev*	*+1.9*	*-1.9*	*-1.1*		*+1.2*		*-1.3*	*+1.3*
MTNP	Exp. 293K	11.921	8.339	8.476				842.61	1.711
$Pna2_1$	PBE-D2	11.797	8.267	8.480				826.98	1.744
1056644	*% dev*	*-1.0*	*-0.9*	*+0.0*				*-1.9*	*+1.9*
1CL20:	Exp. 293K	8.351	11.430	11.940		98.66		1126.73	1.932
1MTNP	PBE-D2	8.345	11.450	12.012		98.66		1134.61	1.918
$P2_1$ 1056638	*% dev*	*-0.1*	*+0.2*	*+0.6*		*-0.0*		*+0.7*	*-0.7*

References

[1] Q. Deng *et al.*, "Probing impact of molecular structure on mechanical property and sensitivity of energetic materials by machine learning methods," *Chemometrics and Intelligent Laboratory Systems*, p. 104331, Apr. 2021, doi: 10.1016/j.chemolab.2021.104331.

[2] X. Bidault and S. Chaudhuri, "Improved predictions of thermomechanical properties of molecular crystals from energy and dispersion corrected DFT," *J. Chem. Phys.*, vol. 154, no. 16, p. 164105, Apr. 2021, doi: 10.1063/5.0041511.

[3] B. W. ASAY, B. F. HENSON, L. B. SMILOWITZ, and P. M. DICKSON, "On the Difference in Impact Sensitivity of Beta and Delta HMX," *Energetic Materials*, Jun. 2010, doi: 10.1080/713770434.

[4] S. Zeman, M. JUNGOVÁ, and Q.-L. YAN, "Impact Sensitivity in Respect of the Crystal Lattice Free Volume and the Characteristics of Plasticity of Some Nitramine Explosives," Dec. 25, 2015. http://www.energetic-materials.org.cn/publish_article/2015/12/2015111.htm (accessed Apr. 13, 2021).

[5] A. A. L. Michalchuk *et al.*, "Predicting the reactivity of energetic materials: an ab initio multi-phonon approach," *Journal of Materials Chemistry A*, vol. 7, no. 33, pp. 19539–19553, 2019, doi: 10.1039/C9TA06209B.

[6] A. A. L. Michalchuk, S. Rudić, C. R. Pulham, and C. A. Morrison, "Predicting the impact sensitivity of a polymorphic high explosive: the curious case of FOX-7," *Chem. Commun.*, vol. 57, no. 85, pp. 11213–11216, Oct. 2021, doi: 10.1039/D1CC03906G.

[7] P. A. Banks, Z. Song, and M. T. Ruggiero, “Assessing the Performance of Density Functional Theory Methods on the Prediction of Low-Frequency Vibrational Spectra,” *J Infrared Milli Terahz Waves*, Jun. 2020, doi: 10.1007/s10762-020-00700-7.